

Structural Model of MalK, the ABC Subunit of the Maltose Transporter of *Escherichia coli*

IMPLICATIONS FOR *mal* GENE REGULATION, INDUCER EXCLUSION, AND SUBUNIT ASSEMBLY*

Received for publication, August 16, 2001, and in revised form, October 31, 2001
Published, JBC Papers in Press, November 14, 2001, DOI 10.1074/jbc.M107905200

Alex Böhm, Joachim Diez, Kay Diederichs, Wolfram Welte, and Winfried Boos‡

From the Department of Biology, Universität Konstanz, 78457 Konstanz, Germany

We are presenting a three-dimensional model of MalK, the ABC subunit of the maltose transporter from *Escherichia coli* and *Salmonella typhimurium*. It is based on the recently published crystal structure of the closely related *Thermococcus litoralis* MalK. The model was used to identify the position of mutations affecting the different functions of the ABC subunit. Six *malK* point mutations were isolated specifically affecting the interaction with MalT, the transcriptional regulator of the maltose system. They were mapped on the structural model and define a MalT interaction site that is located on an exposed surface of the C-terminal regulatory domain. Published point mutations that confer an inducer exclusion insensitive phenotype form a patch adjacent to and oriented perpendicularly to the MalT interaction site. Three sequence motifs were identified and visualized that are highly conserved among ABC subunits with extended C termini. They form a subdomain between the regulatory and ATPase domain and might play an important role in signal transduction events between these two domains. Mutations in this domain remain fully active in MalT regulation but cause transport defects. In addition, amino acids that have previously been shown to be involved in the interaction with the transmembranous subunits MalF and MalG and that fall into the highly conserved N-terminal ATPase domain were visualized. The validity of the modeled MalK structure was verified by structure-directed mutagenesis of amino acids located within the proposed MalK-MalT interaction site.

The *Escherichia coli*/*Salmonella typhimurium* maltose transporter is one of the best studied examples for binding protein-dependent ABC transporters. It consists of the periplasmic high affinity maltose-binding protein (MBP)¹; two homologous transmembrane proteins, MalF and MalG, that form a heterodimeric pore; and two copies of the ATPase subunit MalK that are cytoplasmically associated with the pore-forming subunits (1, 2). Interaction between MalF/G and MalK

was shown by a combination of genetic and biochemical studies to involve the so-called EAA loop, a sequence motif that is present in all MalF/G homologues and a number of residues that are conserved in MalK and its homologues (3, 4). Recently, the crystal structure of the MalK protein from the hyperthermophilic archaeon *Thermococcus litoralis* has been solved (5). The *T. litoralis* MalK sequence is 47% identical to *E. coli* MalK. The protein was shown to consist of two domains; the N-terminal 3/5 of the protein form an α/β type ATPase domain that is present in all ABC proteins, whereas the C-terminal 2/5 of the protein form a barrel-like structure that is present in only a subset of all bacterial and archaeal ABC transporters in the data bases. From studies with the *E. coli* and *S. typhimurium* maltose system, this C-terminal domain is thought to represent the interaction site with regulatory proteins and is thus called the regulatory domain.

According to a model proposed by Diederichs *et al.* (5), which is in agreement with very recent findings by Chen *et al.* (6), maltose uptake is thought to involve a series of conformational changes and signal transduction events; when substrate-loaded MBP docks to its cognate sites on the periplasmic lobes of the MalF/G subunits, a conformational change takes place that virtually abolishes the high affinity substrate binding of MBP and at the same time leads to channel opening. This allows maltose to diffuse through the MalF/G pore and enter the cytoplasm. ATP hydrolysis is then needed to release substrate-free MBP from the transporter complex and to close the channel. After uptake, maltodextrins are degraded by three enzymes to glucose and glucose-1-phosphate. A by-product of dextrin metabolism is maltotriose, the inducer of the system that stimulates the transcriptional activator of the system, the MalT protein (7). In addition to this classical regulation scheme, MalT activity is also modulated by MalK. It has been shown *in vitro* and *in vivo* that both proteins can interact (8), that MalK can abolish MalT-dependent transcription when overexpressed (9), and that *malK* null mutants become constitutive for *mal* gene expression (10). One model for the physiological role of this phenomenon proposes that MalT constantly samples the transport state of the maltose transporter. When no substrate is being transported, MalT is bound to the MalFGK₂ complex *via* MalK, and *mal* gene transcription cannot occur (2, 11).

MalK not only exerts repression on MalT but is also subject to inactivation in a process known as inducer exclusion; in *E. coli* and *S. typhimurium* glucose is transported *via* the phosphotransferase system (PTS). During transport glucose is phosphorylated, which leads in a series of phosphotransfer reactions to dephosphorylation of the EIIA^{Glc} protein. EIIA^{Glc} plays a central role for the regulation of non-PTS sugar uptake systems, such as the *lac* permease, the melibiose permease, and the maltose ABC transporter (12). In its dephosphorylated

* This work has been supported by grants from the Deutsche Forschungsgemeinschaft and the Fonds der Chemischen Industrie. The costs of publication of this article were defrayed in part by the payment of page charges. This article must therefore be hereby marked "advertisement" in accordance with 18 U.S.C. Section 1734 solely to indicate this fact.

‡ To whom correspondence should be addressed. Tel.: 49-7531-882658; Fax: 49-7531-883356; E-mail: Winfried.Boos@Uni-Konstanz.De.

¹ The abbreviations used are: MBP, maltose-binding protein; PTS, phosphotransferase system; α -MG, α -methylglucoside; cam, chloramphenicol; IPTG, isopropyl- β -D-thio-galactopyranoside; RDM, regulatory domain motif; wt, wild type.

form EIIA^{Glc} inhibits uptake of non-PTS substrates by direct interaction with the various transport proteins. It has been shown, mostly by genetic studies, that MalK is the target of inducer exclusion exerted on the maltose ABC transporter. There are a number of point mutants that have been isolated in a selection for resistance against α -methylglucoside (α -MG), a nonmetabolizable glucose analogue that is transported and phosphorylated by the PTS, leading to strong inducer exclusion and thus leading to a Mal⁻ phenotype (13, 14). Because mutations in *malK* that affect inducer exclusion do not interfere with MalT inactivation, it is very likely that MalK possesses two distinct binding sites for MalT and EIIA^{Glc}.

Because all mutations affecting the different functions of MalK have been isolated in *E. coli* or *S. typhimurium* MalK (which is practically identical to *E. coli* MalK), we have used homology modeling to obtain an atomic structure of this protein. The model is based on the structure of *T. litoralis* MalK and a multiple sequence alignment of 60 bacterial and archaeal ABC ATPases that possess a regulatory domain.

EXPERIMENTAL PROCEDURES

Bacterial Strains and Plasmids—Strains used in this work are derivatives of *E. coli* K-12. Bre1162 (15) is a derivative of MC4100 (16) and has a transcriptional *malK-lacZ* fusion that confers a Mal⁻ phenotype. RP526 (17) carries the *mutD5* allele and was used for *in vivo* mutagenesis. Plasmid pMR11 (9) is a pACYC184 derivative and carries the *malK* gene under a constitutive *P_{trc}* promoter. Plasmids pAB201 and pAB204 have been created by standard PCR cloning techniques and are pBR322 derivatives that carry the *lacI^r* allele for control of a *P_{tac}* promoter under which a C-terminal part of MalK (corresponding to the C-terminal 156 amino acids; pAB201) or full-length MalK (pAB204) is expressed. Strains were grown in LB medium or in minimal medium A (18) supplemented with 0.2% maltose or 0.4% glycerol. MacConkey indicator plates contained 1% maltose. Chloramphenicol (cam), nalidixic acid, and ampicillin were added to final concentrations of 30, 40, and 100 μ g/ml, respectively. For induction of pAB204-derived MalK, isopropyl- β -D-thio-galactopyranoside (IPTG) was added to a final concentration of 10 μ M.

Molecular Biology Techniques—To identify point mutations in pMR11 encoded *malK* alleles, *DraIII/SacII* restriction fragments of *malK* were subcloned, and the resulting plasmids were checked for their maltose phenotype and their regulatory phenotype. Subsequently, sequencing was carried out at GATC (Konstanz, Germany) on an ABI automated sequencer. Site-directed mutagenesis was carried out essentially as described for the QuikChange kit from Stratagene (La Jolla, CA). In brief, for each point mutation a pair of complementary oligonucleotides (25–30 bases) was ordered from MWG Biotech (Ebersberg, Germany) that encoded the desired mismatch. These oligos were used as primers for 14 cycles of *in vivo* DNA replication of the entire plasmid (pAB204) with Pwo polymerase from pEQLab (Erlangen, Germany). Subsequently, methylated template DNA was removed with a *DpnI* restriction, and the entire mixture was electroporated into DH5 α cells. To confirm the introduction of the desired mutations, sequencing of individual plasmid clones was carried out as above. Standard DNA techniques were according to Sambrook *et al.* (19).

β -Galactosidase Assays—Overnight cultures of strain Bre1162 harboring plasmids encoding wild type or mutant MalK were diluted 1:30 into fresh minimal medium A (containing glycerol and cam or ampicillin) and grown to mid-log phase. For induction of MalK of pAB201/204-derived plasmids, IPTG was added to a final concentration of 10 μ M. Cell disruption was carried out with chloroform and SDS. β -Galactosidase assays were performed at room temperature in microtiter plates as described (20). *ortho*-Nitrophenol production was followed on an Anthos htII plate reader (Anthos Labtec, Salzburg, Austria) at 420 nm and pH 7.1. Each strain was assayed in duplicate and reproduced twice.

Screen for Regulatory Mutants—The *mutD5* strain RP526 was transformed with plasmid pMR11, and the transformants were selected on LB cam plates. From 40 individual colonies overnight cultures (supplemented with cam) were grown, and as a measure of their mutagenicity, the frequency with which nalidixic acid-resistant mutants occurred in these cultures was assessed by plating an aliquot on LB nalidixic acid plates. From 12 cultures that showed the highest mutagenicity, plasmid minipreps were prepared. The *malK-lacZ* strain Bre1162 was electrotransformed with each plasmid pool, and transformants were selected on MacConkey maltose plates containing cam. After overnight growth

Mal⁺ clones were identified as red colonies and purified once; plasmid DNA was prepared and retransformed into Bre1162 to confirm that the mutation conferring the Mal⁺ phenotype is associated with the plasmid.

SDS-PAGE and Western Blots—Individual clones of Bre1162 harboring mutant variants of pMR11 or pAB204 were grown in minimal medium A (supplemented with glycerol and the appropriate antibiotic) to the late logarithmic phase. For clones carrying pAB204-derived plasmids IPTG was added to a final concentration of 10 μ M. The cells were pelleted, resuspended in 1 \times sample buffer, and boiled for 5 min. SDS-PAGE was carried out according to Sambrook *et al.* (19) on 12% gels. To assure loading of equal amounts of total protein, the A_{578} of individual cultures was measured, and the volumes were adjusted accordingly. Subsequently, proteins were transferred to a polyvinylidene difluoride membrane as described (21) and incubated with MalK-specific antiserum. Detection was carried out by a secondary antibody coupled to alkaline phosphatase.

Modeling of the E. coli MalK Three-dimensional Structure—*E. coli* MalK and *T. litoralis* MalK were aligned based on a multiple sequence alignment of 60 bacterial and archaeal ABC transporters that share the regulatory domain, *i.e.* have an extended C terminus (see Fig. 1). The alignment was carried out at the Clustal 1.81 server at *clustalw.genome.ad.jp*. The model of the highly conserved ATPase domain was generated with the help of SWISS-MODEL (22), which modeled the N-terminal 243 residues of *E. coli* MalK against the published three-dimensional structure of *T. litoralis* MalK. The alignment employed by SWISS-MODEL for this domain corresponds to our multiple sequence alignment. The C terminus was generated by manual modeling with the program O (23). As a guide we used the multiple sequence alignment and slightly shifted the positions of deletions and insertions to position them between α -helices and β -strands of the *T. litoralis* MalK structure, thereby avoiding disruption of secondary structure elements. The loop data base of “O” was then used to insert missing residues or to connect ends of segments where deletions occurred. No extensive energy minimization was performed. The model of the *E. coli* MalK dimer was generated accordingly, by building *E. coli* MalK models of chain A and chain B of the *T. litoralis* MalK dimer separately and subsequently assembling both models. The coordinates as Protein Data Bank files are available on request.

RESULTS

E. coli MalK and T. litoralis MalK Have the Same Three-dimensional Structure—*E. coli* and *T. litoralis* MalK both belong to the same class of ABC ATPases (24) and catalyze maltose transport. Despite the fact that these two organisms are evolutionarily distant and have largely different growth temperature optima (37 °C versus 85 °C), their MalK proteins are overall 47% identical and 64% conservatively exchanged in their amino acid sequence and have almost the same number of residues (371 versus 372). Sequence identity is mostly concentrated in the N-terminal ATPase domain up to amino acid 242 (Fig. 1) and less pronounced in the C-terminal regulatory domain. The PHD secondary structure prediction algorithm (25) yields identical results for both proteins (data not shown) that in the ATPase domain are in accordance with the experimentally determined secondary structure of *T. litoralis* MalK. The only exceptions are a 6-amino acid-long deletion in *E. coli* MalK that includes the very short strand $\beta 6$ of *T. litoralis* MalK and a stretch of approximately 50 amino acids that corresponds to the N-terminal part of the regulatory domain. The prediction for the latter region is identical for both proteins, but some of the shorter β -sheets seen in the experimentally determined *T. litoralis* structure were not predicted by the program. The modeling of *E. coli/S. typhimurium* MalK is based on the assumption that the folding of the protein in principle corresponds to the determined structure of *T. litoralis* MalK. Evidence for this assumption comes from a number of facts. Up to now, all available ABC structures (some of them still unpublished) are nearly superimposable in their monomeric form with the *T. litoralis* MalK structure. This includes the HisP protein from *S. typhimurium* (26) and the ABC subunit of a glucose transporter from *Sulfolobus solfataricus* (including the C-terminal regulatory extension) (56). Identical folding of pro-

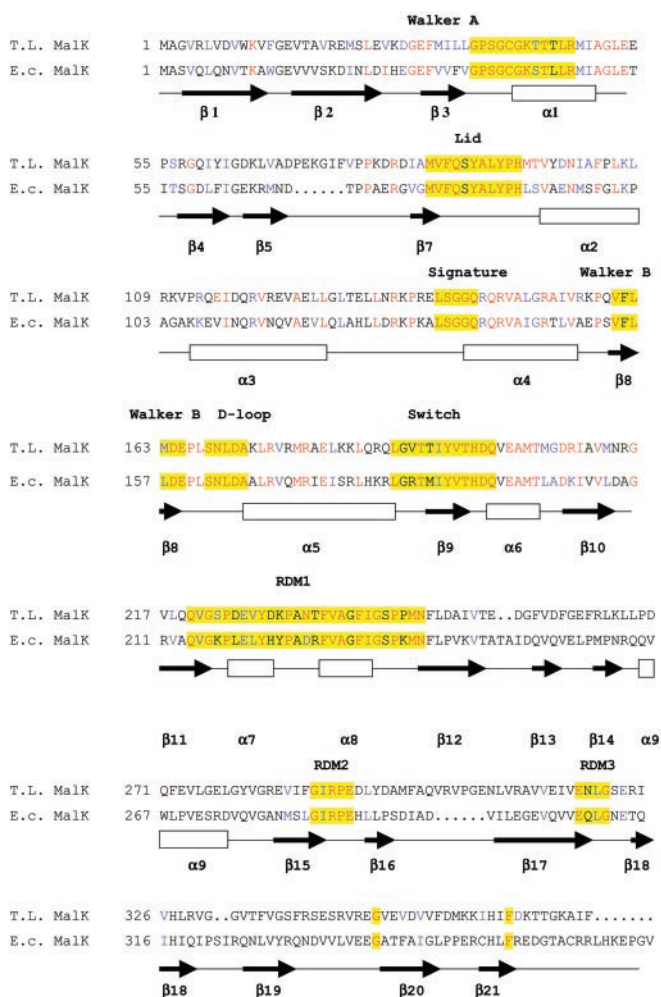


FIG. 1. Alignment of *T. litoralis* MalK with *E. coli* MalK based on an extended sequence comparison. Sequences of 60 nonredundant archaeal and bacteria-binding protein-dependent ABC subunits harboring extended C-terminal extensions were aligned to obtain an optimal alignment between *T. litoralis* MalK and *E. coli* MalK. Amino acids that are more than 70% identical among the 60 sequences are colored red, and amino acids that represent conservative exchanges to more than 70% are colored blue. Conserved motifs (Walker A, Walker B, the signature motif, the Lid, the D loop, the Switch, and the three RDMs) plus two additional amino acids that only occur in ABC subunits with extended C termini are highlighted in yellow. Below the sequences β -strands and α -helices are indicated that have been identified in the structure of *T. litoralis* MalK. The same nomenclature as in Fig. 3 of Diederichs *et al.* (5) is used. The alignment led to the omission of β_6 , which in *T. litoralis* only consists of two amino acids (Ile and Phe). This position, consisting of 6 amino acids, is deleted in *E. coli* MalK, thus shortening the loop between β_5 and β_7 . The other deletions that are revealed in this alignment are two amino acids between β_{12} and β_{13} as well as β_{18} and β_{19} in *T. litoralis* MalK and of six amino acids between β_{16} and β_{17} in *E. coli* MalK.

teins with similar function despite low sequence identity has been recognized for some time and has been used successfully for structural modeling (27–29). For instance, we previously established the crystal structure of TMBP, the trehalose/maltose-binding protein from *T. litoralis*. Despite only 26% sequence identity with the *E. coli* MBP, both proteins are nearly identical in their three-dimensional structure (30). Therefore, we reasoned that also the ABC subunits of the maltose transporters in *E. coli* and *T. litoralis* must indeed share the same three-dimensional structure. Nevertheless, the sequence of *T. litoralis* MalK and *E. coli/S. typhimurium* MalK is not identical, and the placing of small insertions and deletions has to be at the correct position. We used a multiple sequence alignment

of 60 nonredundant bacterial and archaeal ABC transporters that possess a regulatory domain to obtain the most reliable positioning of the *E. coli/S. typhimurium* sequence onto the established structure of the *T. litoralis* protein (Fig. 1). Corroborating the reliability of this alignment is the appearance of three highly conserved motifs and two highly conserved amino acids (Gly³⁴⁰ and Phe³⁵⁵) that were identified in the regulatory domain aside from the well established ABC motifs in the ATPase domain. These C-terminal motifs were termed regulatory domain motifs (RDMs) and fall into the linker region between ATPase domain as well as in the regulatory domain. The alignment revealed that *E. coli* MalK harbors two deletions of six amino acids and two insertions of two amino acids each, when compared with *T. litoralis* MalK. These deletions and insertions are positioned in loops between the conserved α -helices and β -strands, with the exception of β_6 , which is deleted in *E. coli* MalK (Fig. 1). Interestingly, the region around β_6 is also different in the structure of HisP (26), which is otherwise superimposable in its monomeric form with MalK from *T. litoralis*. The alignment shown in Fig. 1 was used to obtain the atomic coordinates of the modeled *E. coli* MalK structure after optimizing the atomic angles and distances in the α -carbon backbone.

The modeled three-dimensional structure of *E. coli* MalK is shown in Fig. 2. In Table I, indicators of structural quality are listed for the modeled structure in comparison with the established structure of *T. litoralis* MalK. As has to be expected for a structure derived from homology modeling, the quality indicators for the *E. coli* MalK model are not as favorable as for the experimentally determined *T. litoralis* MalK structure; however, they are within the ranges of values obtained for well refined experimental structures, at a lower resolution (around 2.5 Å) than that of *T. litoralis* MalK (1.8 Å).

Mutations That Specifically Affect the Regulatory Function of *E. coli* MalK—Strain Bre1162 (*malK-lacZ*) carrying plasmid pMR11 (*malK*⁺) is phenotypically Mal⁻, despite its *mal*⁺ genotype. This is due to overproduction of plasmid-encoded MalK protein, which inhibits any MalT-dependent expression of other *mal* genes. To identify residues that are critical for this regulatory function, we devised a screening method to find mutants that would specifically be affected in the regulatory function but not in the transport-related functions of MalK.

We transformed the *malK* mutant Bre1162 with 12 independently mutagenized plasmid pools and screened about 80,000 transformants for a Mal⁺ phenotype on MacConkey maltose plates (plasmid-encoded wild type (wt) *malK* confers a Mal⁻ phenotype under these conditions). Red, Mal⁺ colonies appeared with a frequency of about 10⁻³. Approximately 50 such colonies that showed a fully Mal⁺ phenotype on MacConkey and minimal maltose plates were isolated, and it was confirmed that the mutation conferring this phenotype was plasmid-associated.

Our screen also led to the accumulation of mutants that showed a reduced MalK expression level, presumably because of “promoter down” mutations or folding defects. To identify these undesired mutants we carried out Western blots of total cell protein with MalK-specific antiserum. Of 50 tested mutants, only 11 showed expression levels that corresponded to the wt control. Eight of these clones were derived from different plasmid pools and subjected to further analysis. Western blots of total cells overexpressing either wt MalK protein or mutant variants are shown in Fig. 3A. To test whether the mutations displayed the expected property of increased MalT-dependent transcription, we measured the specific β -galactosidase activity of the *malK-lacZ* reporter fusion and compared plasmid-encoded *malK* point mutants and one deletion mutant (express-



FIG. 2. **Structural model of *E. coli* MalK.** A ribbon representation of the *E. coli* MalK dimer is shown. The presentation and coloring (blue and yellow for the two monomers) are the same as for the *T. litoralis* MalK structure in Fig. 1A in Diederichs *et al.* (5). α -Helices are numbered in red, and β -strands are in black. Note that $\beta 6$ is not present in *E. coli* MalK. The view is perpendicular to the pseudo-2-fold axis relating the individual monomers and the long axis of the dimer. The coordinates as a Protein Data Bank file are available on request.

TABLE I
Comparison of structural quality between the experimental model (MalK of *T. litoralis*, Protein Data Bank code 1G29) and the homology model (MalK of *E. coli*)

	MalK of <i>T. litoralis</i> (Protein Data Bank code 1G29)	MalK of <i>E. coli</i> (homology model)	References
Resolution	1.8 Å	2.5 Å (estimated)	
Ramachandran plot (statistics)	93.6% core 5.8% allowed 0.5% generously allowed 0.2% disallowed	87.6% core 11.7% allowed 0.6% generously allowed	Refs. 50 and 51
Ramachandran plot (individual residues)	generously allowed: Phe ⁸⁷ , Ala ⁹¹ , Arg ¹⁵⁶ , disallowed: Lys ¹⁵⁷	generously allowed: Glu ²⁵⁷ , Val ²⁷⁵	Refs. 50 and 51
Bond length variability: RMS deviation in bond distances	0.018	0.015	Refs. 52 and 53
Bond angle variability: RMS deviation in bond distances	1.831	2.448	Refs. 52 and 53
Structural average packing Z score			Refs. 53 and 54
All contacts: average/Z score	0.208/1.53	-0.253/-1.52	
BB-BB contacts: average/Z score	0.156/1.13	0.092/0.67	
BB-SC contacts: average/Z score	0.229/1.35	-0.396/-2.09	
SC-BB contacts: average/Z score	0.013/0.25	-0.067/-0.24	
SC-SC contacts: average/Z score	0.128/1.02	-0.413/-1.96	
Overall structure estimation: Morris <i>et al.</i> class	112	122	Refs. 50 and 55

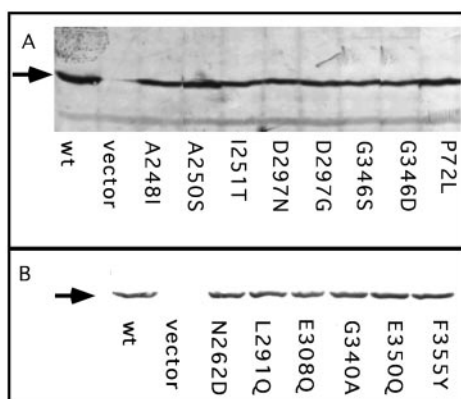


FIG. 3. **Mutant and wt MalK proteins were synthesized in equal amounts.** Western blots of total cells with MalK specific anti-serum. Equal amounts of total cells were loaded. The arrows indicate the bands that correspond to MalK. A, *malK* mutants screened for regulatory defects. MalK was expressed from the constitutive promoter on pMR11. B, *malK* mutants constructed as deduced from the structure. MalK was expressed from the IPTG-inducible promoter on pAB204 (10 μ M IPTG).

ing the C-terminal 156 amino acids of *E. coli* MalK) to wt *malK*. Although high level expression of wt *malK* or the deletion mutant completely abolished the activity of the *malK-lacZ* fusion, all point mutants allowed transcription from the *malK* promoter. β -Galactosidase activities of the *malK-lacZ* reporter

fusion of the various point mutants were between 10 and 50% of the control strain that expresses no MalK protein (Fig. 4A). All plasmid-encoded MalK mutant proteins allowed growth on minimal maltose plates, indicating that no cross-defect in transport activity had occurred.

Mutations That Cause a Regulation Minus Phenotype Define the MalT Interaction Patch on the Regulatory Domain of MalK—Subcloning and subsequent sequencing revealed that all eight mutants have a single amino acid substitution (Table II). In addition, one more mutation (W267G) conferring this phenotype had been published previously (14). Two pairs of mutants were affected in the same amino acid but carried different substitutions (G346(S/D) and D297(N/G)), and G346S has been reported before (14). Except for P72L, all mutations affect residues that are in the C-terminal domain of MalK. These C-terminal mutations fall into four different regions of the primary structure that are not conserved among ABC ATPases. When the side chains of the mutated amino acids are highlighted on the three-dimensional structure of MalK, most are located at the peripheral face of the regulatory domain that is turned away from the N-terminal ATPase domain (Fig. 5). The patch consists mainly of polar residues that form an irregularly shaped cleft-like structure. Both subdomains, which together form the regulatory domain (5), contribute residues to this surface element. We propose that this structure is the site in MalK that interacts with MalT.

Among the regulatory mutations G346(S/D) is an exception.

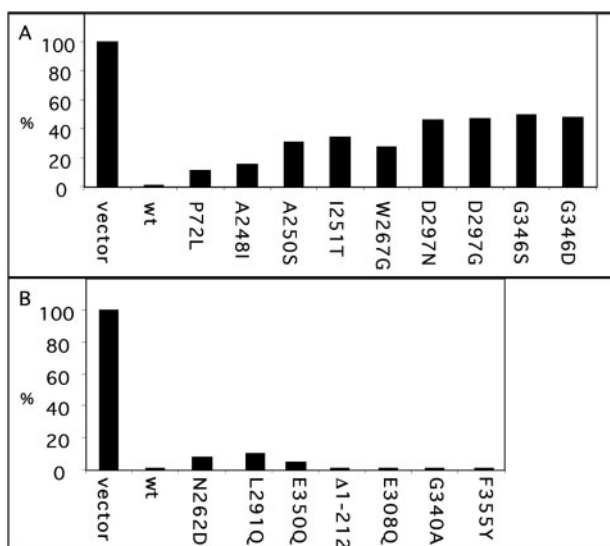


FIG. 4. Repression of *mal* gene expression by mutant MalK proteins. β -Galactosidase activity of strain Bre1162 (*malK-lacZ*) overexpressing wt MalK or different mutant MalK proteins is shown. The activity is given as a percentage of the vector control. For pAB204-derived vectors (B), IPTG was added to a final concentration of 10 μ M to induce protein expression.

It is not surface-exposed but is in close proximity to Asp²⁹⁷, and a mutation to Ser or Asp is easily imaginable to cause local disruptions of the secondary structure that is necessary for interaction with MalT. The P72L mutation is another exception because it displays a regulation negative phenotype but is located in the ATPase domain. Pro⁷² is conserved in the *T. litoralis* MalK protein and resides in a large loop between β -sheets 5 and 7 (Fig. 2). In the *T. litoralis* dimer it is located in the dimer interface where the two proline residues are in close proximity to each other. This proline residue may be instrumental in relocation of the regulatory domain, which in the wt protein is presumed to decrease the affinity for MalT.

Structure-directed Mutagenesis of MalK—To test the validity of the modeled structure of *E. coli* MalK, we changed amino acids in the regulatory domain that were predicted from the three-dimensional model to participate in the interaction with MalT. These exchanges were N262D at the end of β 14, L268Q at the beginning of α 9, L291Q at the beginning of β 16, and E350Q in the loop between β 19 and β 20 (Figs. 1, 2, and 5 for positioning). N262D, L291Q, and E350Q exhibited a weak regulatory phenotype (Fig. 4B), whereas L268Q appeared strongly defective in regulation (not shown in Fig. 4B). This mutation, however, was omitted from further experiments because the amount of protein produced was significantly lower than for the wt protein, whereas the protein amounts of the other three mutants were indistinguishable from wild type expression levels (Fig. 3B). All three mutants appeared to be normal in maltose transport as judged from complementation studies on McConkey indicator plates. The structure-directed mutagenesis clearly demonstrates the validity and the usefulness of the model. It is noteworthy that the regulatory function of MalK is strongly dependent on its expression level. Therefore, for testing the structure-directed mutations we replaced pMR11, which expresses MalK from a strong constitutive promoter, with the inducible plasmid pAB204. This allowed us to observe even weak regulatory effects at appropriately adjusted expression levels (10 μ M IPTG) that could not have been observed with pMR11-derived MalK.

Residues That Are Affected in α -MG-resistant MalK Mutants Define the EIIA^{Glc} Interaction Site—There are two publications describing a class of point mutations in MalK that enable the

respective mutants to transport maltose under conditions of strong inducer exclusion (in the presence of α -MG). Dean *et al.* (13) have found the following mutations to cause an α -MG-resistant phenotype: A124T, F241I, G278P, and G284S, whereas Kühnau *et al.* (14) have found E119K, R228C, G302D, and S322F (Table II). It has been proposed that these MalK variants are affected in the binding of the dephosphorylated form of EIIA^{Glc} and that the interaction site in MalK is conserved among a wide variety of proteins that are subjected to inducer exclusion (13, 31). Six of eight α -MG resistance-causing mutations fall into the regulatory domain of MalK. As for the MalT regulation minus mutations, five α -MG-resistant mutations define an area on the surface of the protein. Residues Phe²⁴¹, Gly³⁰², Arg²²⁸, and Ser³²² participate to form an irregularly shaped surface, whereas Gly²⁷⁸ is not in very close proximity to this structure, albeit on the same face of the regulatory domain and also surface-exposed (Fig. 6). We propose that these five mutations define the site of MalK that interacts with the EIIA^{Glc} protein. The interaction site is on a face of the regulatory domain that is roughly perpendicular to the MalT interaction site as well as to the ATPase domain. Another mutation in the regulatory domain that leads to α -MG resistance (G284S) is affecting a highly conserved residue that is part of RDM2 (see below) but not surface-exposed. Two additional mutations (A124T and E119K) have been described (13, 14) that cause inducer exclusion insensitivity; however, the affected residues are in the helical part of the ATPase domain. Glu¹¹⁹ is at the end of α -helix 3 in close contact with Ala¹²⁴, and both mutations are in the vicinity of the ABC signature motif. Mutations in these amino acids may affect intramolecular signal transduction events that connect EIIA^{Glc} interaction to ATPase activity.

Interaction between ATPase and the Regulatory Domain Involves the Highly Conserved RDMs—We have identified three highly conserved motifs that were termed RDM (Fig. 1) and are only present in nucleotide-binding proteins that possess a regulatory C-terminal domain. When the residues that contribute to these motifs were visualized on the model of *E. coli* MalK, it appeared likely that RDM1 (consisting mainly of α -helices 7 and 8 of the ATPase domain) may contact RDMs 2 and 3, as well as the highly conserved phenylalanine 355 of the regulatory domain (Fig. 7) by a hinge motion. Thus, these motifs appear to represent communication modules between the two domains of MalK-type ATPases. Interestingly, RDM1 is also in close contact with the conserved α -helix 6, which follows the switch region.

To give evidence for the important role of the newly described RDMs, we changed amino acids within the RDM region located within the C-terminal extension of MalK. We chose positions that were furthest away from the ATPase domain of the protein. E308Q (within β 17) is part of RDM3, and G340A (positioned in the loop between β 19 and 20) and F355Y (within β 21) are single, highly conserved amino acids at the extreme C terminus of MalK (Fig. 1). Of these mutant MalK proteins, E308Q was no longer able to complement a *malK* null mutation for a red phenotype on McConkey maltose plates, whereas G340A and F355Y display an intermediate light pink phenotype on McConkey plates that is clearly distinguishable from wt (data not shown). These mutant MalK proteins were fully active as MalT regulators and produced the same protein amounts as wt MalK (Fig. 3B). This demonstrates that the RDMs are not merely a motif that facilitates proper folding of the regulatory domain but play an important role for substrate translocation.

Residues Involved in the Interaction of MalK with the Membrane Components—By suppressor mutation studies, Mourez

TABLE II
Summary of mutations in *E. coli* or *S. typhimurium* malK that are the subject of this work

Mutations, their location (secondary structure element), phenotype, and reference are given. “↔” indicates that the particular residue is located in a loop region between two secondary structural elements.

Mutations in <i>malK</i>	Maps to	Phenotype	Reference
Ala ⁸⁵ → Met	β7 ↔ α2 (the Lid)	suppressor of EAA loop mutation and cross-linkable to EAA loop after change to Cys	Ref. 3
Val ¹¹⁷ → Met	α3		Ref. 4
Val ¹⁴⁹ → Met/Ile	α4	suppressor of EAA loop mutation	Ref. 3
Lys ¹⁰⁶	α3	cross-linkable to EAA loop after change to Cys	Ref. 4
Val ¹¹⁴	α3		
Ala ¹²⁴ → Thr	α3 ↔ α4		Ref. 13
Phe ²⁴¹ → Ile	β12	Inducer exclusion insensitivity	
Gly ²⁷⁸ → Pro	α9 ↔ β15		
Gly ²⁸⁴ → Ser	β15		
Glu ¹¹⁹ → Lys	α3		Ref. 14
Arg ²²⁸ → Cys	α8	Inducer exclusion insensitivity	
Gly ³⁰² → Asp	β17		
Ser ³²² → Phe	β18 ↔ β19		
Trp ²⁶⁷ → Gly	α9	MalT regulation negative	Ref. 14
Gly ³⁴⁶ → Ser	β20		
Pro ⁷² → Leu	β5 ↔ β7		
Ala ²⁴⁸ → Ile	β12 ↔ β13		
Ala ²⁵⁰ → Ser	β12 ↔ β13	MalT regulation negative	This work
Ile ²⁵¹ → Thr	β12 ↔ β13		
Asp ²⁹⁷ → Asn/Gly	β16 ↔ β17		
Gly ³⁴⁶ → Asp/Ser	β20		
Asn ²⁶² → Asp	β14	MalT regulation negative; from structure-directed mutagenesis	This work
Leu ²⁶⁸ → Gln	α9		
Leu ²⁹¹ → Glu	β16		
Glu ³⁵⁰ → Gln	β19 ↔ β20		
Glu ³⁰⁸ → Gln	β17	Part of the RDM subdomain; defective in maltose utilization	This work
Gly ³⁴⁰ → Ala	β19 ↔ β20		
Phe ³⁵⁵ → Tyr	β21		

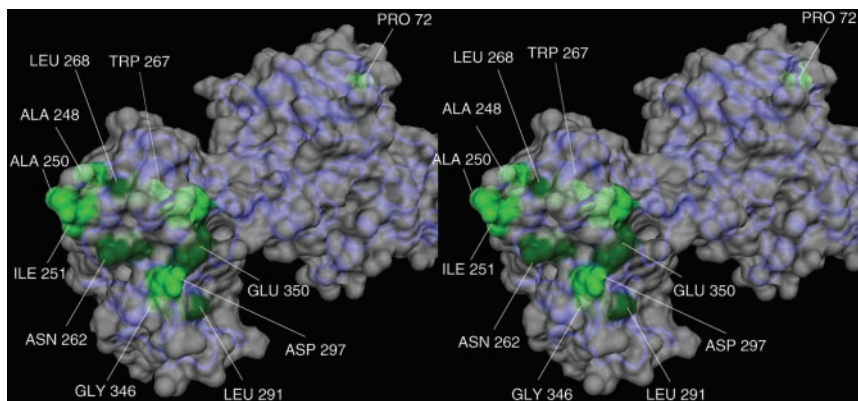


FIG. 5. **The MalT interaction site.** A stereo representation of the model of monomeric *E. coli* MalK is shown. Shown in blue is the α -carbon ribbon of the molecule. The Van der Waals' surface of the protein is represented as a gray translucent surface. Highlighted in green are amino acids that cause a regulatory phenotype when mutated. Light green indicates that the residue is buried (Gly³⁴⁶, Trp²⁶⁷, and Pro⁷²) or partly turned away from the chosen view (Ala²⁴⁸). Dark green indicates amino acid positions that were chosen for mutagenesis from their location within the putative interaction patch (Asn²⁶², Leu²⁶⁸, Leu²⁹¹, and Gly³⁵⁰). The view is onto the regulatory domain and perpendicular to the pseudo-2-fold axis and at an angle of $\sim 70^\circ$ to the long axis of the dimer with the helical region at the bottom (Fig. 2). Note the position of Pro⁷² in the ATPase domain.

et al. (3) have identified residues that are involved in the interaction of MalK with MalF and MalG. Mourez *et al.* proposed that MalK docks to the so-called EAA loop that is conserved among members of the MalF/G family. Amino acids in MalK that are involved in EAA loop interaction were shown to be Ala⁸⁵, Val¹¹⁷, Val¹⁴⁹, Val¹⁵⁴, and Met¹⁸⁷. The latter two were only complementing when overexpressed, requiring an unknown secondary mutation. Because of their complex behavior they are omitted from this analysis. By cysteine cross-linking experiments, Hunke *et al.* (4) have confirmed Ala⁸⁵ and Val¹¹⁷ and identified two additional residues (Lys¹⁰⁶ and Val¹¹⁴) that are probably in close contact with the membrane components. From these experiments it is clear that the α -helical region of the ATPase domain is critical for interaction with the trans-

membranous components. Because MalK occurs as a dimer in the intact transport complex, it is desirable to map the amino acids relevant for the interaction with the membrane components in the dimeric structure of MalK. We used the dimeric form of the *T. litoralis* protein as a model for the *E. coli* dimeric structure (Fig. 2). The strongest argument for the validity of this operation is the ability of Ala⁸⁵, when changed to cysteine, to cross-link the dimer (4). When the “interaction residues” are highlighted on the structure of the dimeric ATPase domain, only Ala⁸⁵ is part of the dimer interface, but others (Lys¹⁰⁶ being an exception) are deeply buried in the monomeric molecule (Fig. 8). Surprisingly, most of these residues are accessible through a deep tunnel that has its entry on the face of the molecule that consists of β -sheets. The tunnel-like structure is

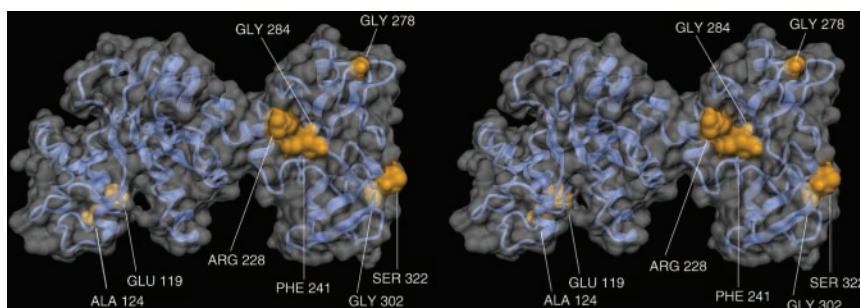


FIG. 6. **The EIIA^{Glc} interaction site.** A stereo representation of the model of monomeric *E. coli* MalK is shown. The view is perpendicular to the long axis and the pseudo-2-fold axis of the dimer (as in Fig. 2). The α -carbon trace is shown in *blue* in the ribbon representation; the Van der Waals' surface of the protein is shown in *translucent gray*. Positions of amino acids that cause an α -MG-resistant (inducer exclusion insensitive) phenotype when mutated are highlighted in *gold*; *light gold* indicates that the residue is buried (Gly²⁸⁴) or surface-exposed on the opposite side of the molecule (Glu¹¹⁹ and Ala¹²⁴) or away from the chosen view (Gly³⁰²).

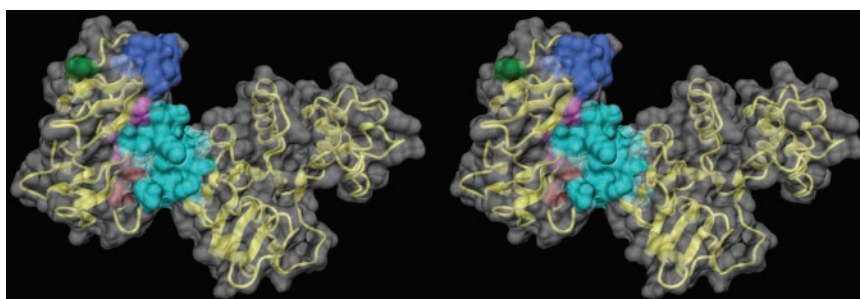


FIG. 7. **The interaction between the regulatory and ATPase domains.** A stereo view of the model of monomeric *E. coli* MalK is shown. The view is perpendicular to the long axis of the dimer and from below (Fig. 2) at an angle of $\sim 30^\circ$ relative to the pseudo-2-fold axis. The α -carbon backbone is shown in *yellow* in the ribbon representation, and the Van der Waals' surface of the protein is shown in *translucent gray*. The individual RDMs and two highly conserved residues are highlighted in the following colors: RDM1 in *cyan*, RDM2 in *purple*, RDM3 in *blue*, Phe³⁵⁵ in *red*, and Gly³⁴⁰ in *green*.

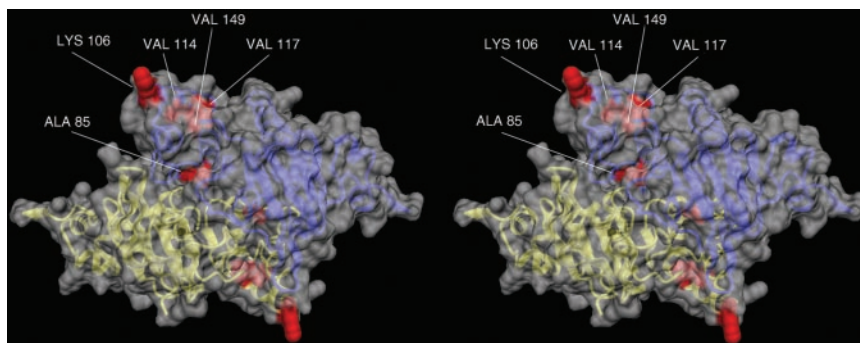


FIG. 8. **Positioning of amino acids known to interact with the membrane components MalF and MalG.** A stereo representation of the model of dimeric *E. coli* MalK is shown; only the N-terminal ATPase domains are shown. The α -carbon backbones are shown as ribbons of the individual monomers in *yellow* and *blue*. The Van der Waals' surfaces of the proteins are *translucent gray*. Positions of amino acids that are involved in the interaction with the transmembrane subunits are highlighted in *red* in both monomers, and their nature and position in the primary structure are indicated for the *blue* monomer only. The view is perpendicular to the long axis of the dimer but at an angle of $\sim 30^\circ$ relative to the pseudo-2-fold axis and onto the β -sheet region of the protein (from the *top* in relation to Fig. 2). The tilting against the pseudo-2-fold axis allows a better view into one of the two tunnels (see text).

in part formed by residues that were shown to be involved in the interaction with MalF/G and has Ala⁸⁵ at its deepest end. From the mouth of the tunnel, α -helix 3 protrudes, with Lys¹⁰⁵ (highly conserved) and Lys¹⁰⁶ (not conserved) at its tip. Lys¹⁰⁶ was shown to be cross-linkable with MalF/G (4), and its susceptibility to trypsin cleavage was shown to change in the presence of ATP and MalF/G (32). In the MalK homodimer the two tunnels are in relative positions to each other that resemble a "straddled" V. Both Ala⁸⁵ residues, which are part of the lid, are in close proximity to each other at the bottom of the V, and the Lys¹⁰⁶ residues are in great distance from each other and form the top of the V-like structure. The highly conserved lid region is directly underneath this putative MalF/G interaction site, and it is conceivable that conformational changes in

the lid region might have direct consequences for the transmembranous subunits (Fig. 9).

DISCUSSION

We present a three-dimensional model for *E. coli*/*S. typhimurium* MalK to combine data obtained by the powerful genetic techniques available for *E. coli* and *S. typhimurium* with structural information obtained from MalK of the hyperthermophilic archaeon *T. litoralis*. The validity of the modeled three-dimensional structure is high. It is based on the overwhelming body of evidence that proteins of analogous functions even with a rather low level of sequence identity exhibit nearly the same three-dimensional folding (27–29). One of the most striking examples for this conclusion is the structural identity

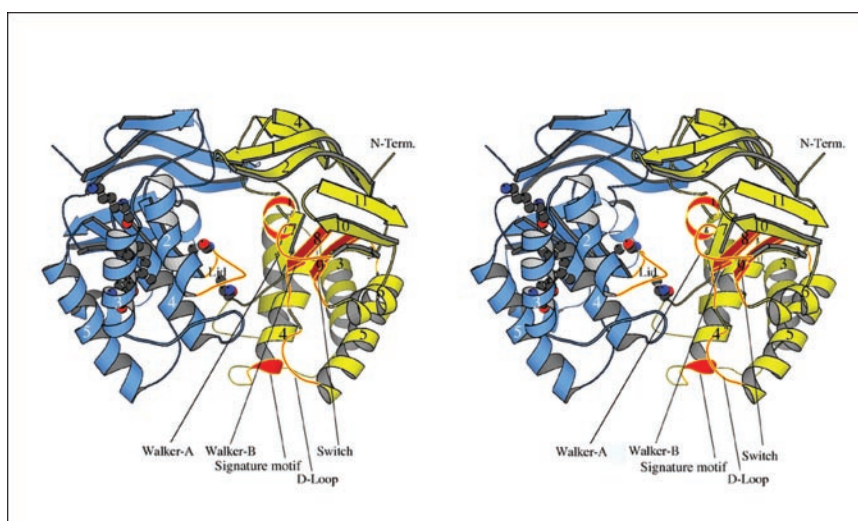


FIG. 9. Position of amino acids known to interact with the membrane components MalF and MalG shown in relation to conserved ABC motifs. The stereo view along the interface perpendicular to the 2-fold axis (Fig. 2) of the ATPase domain only is shown. From top to bottom the three layers of the dimeric molecule are seen: antiparallel sheet; mixed sheet with P loop and helix 1 (the Walker A motif); and the helical layer. Coloring is as in Fig. 2 except that the conserved regions from the yellow monomer (Walker A, Walker B, Signature motif, D loop, and Switch) as well as the lid from the blue monomer are marked in red. Labels indicate the numbers of strands and helices according to the numbering in Fig. 2. Amino acids Lys¹⁰⁶, Val¹¹⁴, Val¹¹⁷, and Val¹⁴⁹, experimentally found to interact with the membrane components MalF/G, are indicated in their correct orientations in ball and stick representation (gray, carbon; red, oxygen; blue, nitrogen) only in the blue monomer. Ala⁸⁵ of the Lid region known to interact with MalF/G as well as to cross-link MalK after changing to cysteine is shown in both monomers.

of the many different periplasmic substrate-binding proteins (33). Also, the crystal structure of the HisP monomer of *S. typhimurium*, another ABC protein, is nearly identical to the N-terminal ABC domain of *T. litoralis* MalK, despite the relatively low sequence similarity (30% identical and 55% conservatively exchanged residues) (26). Interestingly, the only deviation between the N-terminal domains of *T. litoralis* MalK and *S. typhimurium* HisP (around β -strand 6 of *T. litoralis* MalK) coincides with the only significant difference between the *E. coli* MalK model and *T. litoralis* MalK structure. Apparently, this region is variable among the various members of the group of nucleotide-binding proteins. The validity of the *E. coli* MalK model is corroborated by the secondary structure prediction for the *E. coli* and *T. litoralis* MalK proteins, which (with the exception of β 6) are nearly identical and match the experimentally determined secondary structure of *T. litoralis* MalK. Nevertheless, small alterations in the amino acid sequence (deletions and insertions) between the *E. coli* and *T. litoralis* sequence had to be placed correctly to obtain an optimal match between the two structures. Therefore, we used a multiple alignment of 60 nonredundant prokaryotic ABC sequences with extended C termini. The validity of this alignment is born out not only by the appearance of all known ABC motifs but also by the appearance of highly conserved sequences in the C-terminal portions of the molecules (now called RDMs), part of which have been recognized previously in other alignments (34) (5). The optimal alignment shown in Fig. 1 was used to model the three-dimensional atomic coordinates of the *E. coli* MalK structure (Fig. 2). The usefulness and validity of these coordinates was demonstrated by targeted mutagenesis; based on the three-dimensional model we were able to identify residues that are involved in the regulatory function of MalK. These residues would have been very difficult to identify in a random screen for mutants because of a relatively weak phenotype.

The MalK-MalT Interaction Patch—A clear result was obtained when the positions of the regulatory mutations were visualized on the *E. coli* MalK structure (Fig. 5). Even though the nine affected amino acids in the regulatory domain are separated into several different regions of the primary struc-

ture, they come together in the three-dimensional model to form a cleft-like structure on opposite front faces of the dimeric protein. Obviously, this must be the MalT interaction site. Because the activation of MalT is accompanied by oligomerization (7) and binding of MalT to MalK causes inactivation of MalT, it is likely that two copies of MalT bind as monomers to the assembled MalF/G/K₂ complex *via* the regulatory domains of the MalK subunits.

Pro⁷², the alteration of which also causes a regulatory phenotype, is not in the regulatory domain and not surface-accessible in the MalK homodimer. This residue in the *E. coli* MalK structure as well as in the *T. litoralis* MalK is located in the dimer interface (5). How can a mutation of Pro⁷² still cause a regulation negative phenotype? Maltose transport is thought to involve a complex signal transduction cascade that is triggered by docking of substrate-loaded MBP to MalF/G and ultimately leads to substrate translocation and ATP hydrolysis by MalK. Treptow and Shuman (35) and Covitz *et al.* (36) reported a class of mutations in MalF/G that allow maltose transport in the absence of MBP. These MBP-independent mutants display a partial constitutivity for MalT-dependent transcription. This suggested that the MBP independence as well as the partial constitutivity is brought about by constant ATP hydrolysis of the MalK subunit, which in turn originates from a signal transduction defect that mimics the MBP bound state of the maltose transporter (37). It is conceivable that Pro⁷² plays a role in this signal transduction chain and, like the MBP independent mutations, mimics the MBP-bound state. It would be interesting to study the ATPase activity of the reconstituted complex to see whether or not the ATPase activity in this mutant is uncoupled from MBP.

We showed that the expression of the liberated regulatory domain causes *mal* gene repression (Table II). In addition, Schmees and Schneider (38) have shown that expression of a slightly larger peptide (consisting of the C-terminal 193 residues of *S. typhimurium* MalK) causes half-maximal *mal* gene repression. This is in agreement with a model where the regulatory domain of the transporting ABC transporter is inaccessible for an interaction with MalT, whereas the regulatory domain of the resting transporter is accessible for MalT. There

are at least two ways to picture this event. In the first, the regulatory domain itself is rigid, but its position in relation to the ATPase domain is variable. During transport, repositioning of the regulatory domain would leave it sterically unapproachable for an interaction with MalT. This is reminiscent of elongation factor EF-Tu, where a β -barrel like domain is relocated upon ATP hydrolysis (39). Alternatively, the two subdomains of the regulatory domain could undergo a conformational change during transport, altering their proper arrangement for binding of MalT.

Do MalY and MalK Utilize a Similar Structure to Bind MalT?—MalY is an *E. coli* enzyme exhibiting cystathionase (β -CS-lyase) activity (40) and has been shown to inhibit MalT-dependent transcription activity by binding to the monomeric form of MalT (41). The crystallization of MalY revealed the MalT interaction site (42). The latter can be described as a convex patch of hydrophobic residues that are surrounded by highly polar residues. This structure does not resemble the MalT interaction site of MalK that we present here. Also, there is no detectable sequence similarity between MalY and MalK. These observations argue for the presence of two different binding sites in MalT for MalY and MalK. Nevertheless, from the observation that two monomeric MalT molecules bind a dimeric MalY protein, it appears likely that the same stoichiometry holds true for the MalK-MalT interaction.

EIIA^{Glc}-mediated Inhibition of the Maltose Transporter Might Involve the RDMs and Two Residues in the ATPase Domain—Most of the mutations causing inducer exclusion insensitivity are in the regulatory domain. As for the MalT interaction patch, they define a surface area in the regulatory domain that is, however, positioned roughly perpendicular to the MalT interaction site.

Glu¹¹⁹ and Ala¹²⁴ are not in the regulatory domain but in the helical region of the ATPase domain. How can their alteration cause an α -MG-resistant phenotype? Because both residues are surface-exposed and are in close proximity to each other, it appears at first possible that they contribute to EIIA^{Glc} binding. Given the small size (18 kDa), the globular shape of EIIA^{Glc}, and the considerable distance between the putative EIIA^{Glc} interaction patches in the regulatory domain and the ATPase domain of *E. coli* MalK, one would have to postulate that EIIA^{Glc} has two interaction sites for MalK that are on opposite surfaces of the protein. Feese *et al.* (43, 44) and Hurley *et al.* (45) propose in a number of papers where they report the co-crystallization of EIIA^{Glc} with glycerol kinase that EIIA^{Glc} associates with its various target proteins *via* one hydrophobic patch that surrounds the active site histidine residue. Glycerol kinase utilizes a protruding α -helix to bind EIIA^{Glc}. We have failed to detect any sequence or structural similarities between this α -helix of glycerol kinase and MalK. Yet, Feese *et al.* (44) proposed that EIIA^{Glc} has a relatively loose target recognition site that is not dependent on a conserved structure. It is unclear how EIIA^{Glc} inhibits maltose transport. But it is reasonable to speculate that EIIA^{Glc} binding interferes with ATP hydrolysis and thus abolishes maltose transport. Therefore, we envision a scenario where mutations of Glu¹¹⁹ or Ala¹²⁴ in the neighborhood of the ABC signature motif overcome an EIIA^{Glc} binding-dependent signal transduction event that normally leads to inhibition of ATP hydrolysis. Another mutation (G284S) affecting inducer exclusion might confer its phenotype by a similar mechanism. Gly²⁸⁴ is not surface-exposed and thus is not accessible for an interaction with EIIA^{Glc} but is part of the highly conserved RDM2. It is conceivable that this mutation interrupts a signal transduction event between the regulatory domain and ATPase domain that involves the RDMs.

Sondej *et al.* (31) have reported consensus binding motifs for

proteins that bind EIIA^{Glc}, among them MalK. Their report is based on experiments with lactose permease (which is subject to EIIA^{Glc}-mediated inducer exclusion) and sequence comparison between lactose permease and other proteins. They propose the existence of two interaction regions. One of them, region II (residues 272–286 in MalK) overlaps largely with the interaction site in the regulatory domain that is defined by α -MG-resistant mutations. Yet, no α -MG-resistant mutations have been found in the putative region I, which is in the ATPase domain and was proposed to consist of the following residues: Val²⁰⁶, Ala²⁰⁹, Arg²¹¹, Gly²¹⁶, and Lys²¹⁷. Even though the putative region I would partly overlap with RDM1, Ala²⁰⁹ and Arg²¹¹ would be located on opposite faces from Gly²¹⁶ and Leu²¹⁷, whereas Val²⁰⁶ would be buried. Thus, we find no compelling evidence that region I of *E. coli* or *S. typhimurium* MalK contributes to EIIA^{Glc} binding. From the work of van der Vlag *et al.* (46), who observed cooperative inhibition of maltose uptake by increasing EIIA^{Glc} concentration, one may conclude that two molecules of EIIA^{Glc} have to be bound to the dimeric MalK within the MalF/G/K₂ complex to inhibit transport. It is unclear whether or not MalT and EIIA^{Glc} can be bound to MalK simultaneously. From the location of the respective interaction patch within the regulatory domain it seems possible.

MalK from *T. litoralis* does carry the C-terminal domain that in the *E. coli*/*S. typhimurium* MalK has been identified as regulatory in two ways: active regulation in controlling *mal* gene expression by sequestering the central activator MalT and passive regulation by being subjected to inhibition by EIIA^{Glc}. The archaeon *T. litoralis* does not contain the PTS. Thus, inducer exclusion as observed in *E. coli* does not occur in *T. litoralis*. Also, up to now, there is no indication for a MalT-like homologue in *T. litoralis*. Nevertheless, the regulatory domain including the RDMs is well conserved. As with other ABC subunits harboring an extended C terminus, this structure must be involved in regulation in general. We picture the RDM structure as a link in a signal transduction pathway connecting yet unknown cellular signals to the regulation of transport activity.

Mutating the conserved amino acid Glu³⁰⁸ in RDM3 to Gln, positioned well within the regulatory domain, as well as changing the single highly conserved amino acids Gly³⁴⁰ to Ala and Phe³⁵⁵ to Tyr at the extreme C terminus, affect transport without reducing the ability of the protein to interact with MalT. This is consistent with an active involvement of the RDMs in the transport process. But because only a subclass of ABC transporters possess RDMs, we favor a model in which the RDM region acts as signal transduction module. The particular mutations (being far away from the ATPase domain) actively lock the protein in the inhibited mode, mimicking inducer exclusion. Consequently, this must mean that transport inhibition, for instance initiated by the binding of EIIA^{Glc} to MalK, is an active process mediated via the RDM linker. In contrast, inhibition of MalT by the regulatory domain must be the default setting that is actively overcome by transport. This can be deduced from the observation that the separately expressed regulatory domain strongly interferes with MalT-dependent transcription. At the moment, the available experimental data do not allow us to conclude that RDMs participate in this process as well, even though this appears likely.

Interaction with the Transmembrane Subunits—Diederichs *et al.* (5) have suggested that helices 2 and 3 and the signature motif are involved in the interaction with the transmembrane subunits and that therefore the helical part of MalK faces toward the membrane, whereas the β -sheets face toward the cytoplasm. The basis for their suggestion is that (i) residues 89–140 were shown to be crucial for interaction with MalF/G

(47), (ii) the signature motif might play a role in activating the ATPase activity of MalK upon conformational changes in MalF/G (48), and (iii) two valines (Val¹¹⁴ and Val¹¹⁷) in helix 3 are cross-linkable to MalF/G (4). Here we mapped these mutations that were experimentally shown to be involved in the interaction with the transmembrane components on the *E. coli* MalK structure (3, 4). Surprisingly, we found that most of the mutated residues (Lys¹⁰⁶ being an exception) are not accessible for protein-protein interactions in the dimeric structure. Of those, only Ala⁸⁵ would be surfaced-exposed in the monomer. Instead, these interaction-prone amino acids are buried in the protein and are all in close proximity to a tunnel-like structure (Fig. 8).

It has been suggested that the *T. litoralis* MalK structure that has been used as the template for the *E. coli* MalK structural model represents a “snapshot” of the working ABC transporter subunit and that the *T. litoralis* MalK protein has mobile subdomains (e.g. the helical region) that may undergo large conformational changes (5). Taken together, these observations support a model where the interaction site between MalK and MalF/G changes drastically during the transport process, possibly involving alternating cycles of opening and closing of the MalK dimer interface (6), which in turn could deliver energy for channel opening and closing. The recently published crystal structure of MsbA (49), an ABC transporter of *E. coli*, analogous to multidrug exporters, shows a V-like structure in which the two nucleotide-binding domains are far apart. Chang and Roth (49) suggest that the transport mechanism is based on the opening and closing of this structure. ATP bound to both nucleotide-binding domains in the open structure would represent the high energy form of the transporter. Triggered by substrate binding, the structure would close, causing translocation of substrate, which in turn is followed by ATP hydrolysis. The closed structure (ADP bound to or free of nucleotide) would thus represent the low energy state of the transporter. It is tempting to speculate that the dimeric MalK structure represents the low energy and closed state of the protein.

Acknowledgments—We gratefully acknowledge the contribution of Howard Shuman who several years ago pointed out to us the highly conserved regions at the C terminus of MalK, now termed RDMS. We thank Erika Oberer-Bley for help in preparing the manuscript.

REFERENCES

- Ehrmann, M., Ehrle, R., Hofmann, E., Boos, W., and Schlösser, A. (1998) *Mol. Microbiol.* **29**, 685–694
- Boos, W., and Shuman, H. A. (1998) *Microbiol. Mol. Biol. Rev.* **62**, 204–229
- Mourez, M., Hofnung, M., and Dassa, E. (1997) *EMBO J.* **16**, 3066–3077
- Hunke, S., Mourez, M., Jehanno, M., Dassa, E., and Schneider, E. (2000) *J. Biol. Chem.* **275**, 15526–15534
- Diederichs, K., Diez, J., Greller, G., Müller, C., Breed, J., Schnell, C., Vornhein, C., Boos, W., and Welte, W. (2000) *EMBO J.* **19**, 5951–5961
- Chen, J., Sharma, S., Quicho, F. A., and Davidson, A. L. (2001) *Proc. Natl. Acad. Sci. U. S. A.* **98**, 1525–1530
- Schreiber, V., and Richet, E. (1999) *J. Biol. Chem.* **274**, 33220–33226
- Panagiotidis, C. H., Boos, W., and Shuman, H. A. (1998) *Mol. Microbiol.* **30**, 535–546
- Reyes, M., and Shuman, H. A. (1988) *J. Bacteriol.* **170**, 4598–4602
- Bukau, B., Ehrmann, M., and Boos, W. (1986) *J. Bacteriol.* **166**, 884–891
- Boos, W., and Böhm, A. (2000) *Trends Genet.* **16**, 404–409
- Postma, P. W., Lengeler, J. W., and Jacobson, G. R. (1996) in *Escherichia coli and Salmonella typhimurium: Cellular and Molecular Biology* (Neidhardt, F. C., Curtiss, R., Ingraham, J. L., Lin, E. C. C., Low, K. B., Magasanik, B., Reznikoff, W. S., Riley, M., Schaechter, M., and Umberger, H. E., eds) pp. 1149–1174, American Society of Microbiology, Washington, D.C.
- Dean, D. A., Reizer, J., Nikaido, H., and Saier, M. (1990) *J. Biol. Chem.* **265**, 21005–21010
- Kühnau, S., Reyes, M., Sievertsen, A., Shuman, H. A., and Boos, W. (1991) *J. Bacteriol.* **173**, 2180–2186
- Bremer, E., Silhavy, T. J., and Weinstock, J. M. (1985) *J. Bacteriol.* **162**, 1092–1099
- Casadaban, M. J. (1976) *J. Mol. Biol.* **104**, 541–555
- Liu, J. D., and Parkinson, J. S. (1991) *J. Bacteriol.* **173**, 4941–4951
- Miller, J. H. (1972) *Experiments in Molecular Genetics*, Cold Spring Harbor Laboratory, Cold Spring Harbor, NY
- Sambrook, J., Fritsch, E. F., and Maniatis, T. (1989) *Molecular Cloning: A Laboratory Manual* (Nolan, C., ed) Cold Spring Harbor Laboratory, Cold Spring Harbor, NY
- Slauch, J. M., and Silhavy, T. J. (1991) *J. Bacteriol.* **173**, 4039–4048
- Towbin, H., Staehelin, T., and Gordon, J. (1979) *Proc. Natl. Acad. Sci. U. S. A.* **76**, 4350–4354
- Guxen, N., and Peitsch, M. C. (1997) *Electrophoresis* **18**, 2714–2723
- Jones, T. A., Zou, J. Y., Cowan, S. W., and Kjeldgaard, M. (1991) *Acta Crystallogr. Sect. A* **47**, 110–119
- Saier, M. H. (2000) *Mol. Microbiol.* **35**, 699–710
- Rost, B. (1996) *Methods Enzymol.* **266**, 525–539
- Hung, L.-W., Wang, I. X., Nikaido, K., Liu, P.-Q., Ames, G. F.-L., and Kim, S.-H. (1998) *Nature* **396**, 703–707
- Russell, R. B., and Sternberg, M. J. (1995) *Curr. Biol.* **5**, 488–490
- Sali, A. (1995) *Curr. Opin. Biotechnol.* **6**, 437–451
- CAFASP-1 (1999) *Proteins* **37**, 209–217
- Diez, J., Diederichs, K., Greller, G., Horlacher, R., Boos, W., and Welte, W. (2001) *J. Mol. Biol.* **305**, 905–915
- Sondej, M., Sun, J., Seok, Y.-J., Kaback, H. R., and Peterkofsky, A. (1999) *Proc. Natl. Acad. Sci. U. S. A.* **96**, 3525–3530
- Mourez, M., Jehanno, M., Schneider, E., and Dassa, E. (1998) *Mol. Microbiol.* **30**, 353–363
- Quicho, F. A., and Ledvina, P. S. (1996) *Mol. Microbiol.* **20**, 17–25
- Hunke, S., Landmesser, H., and Schneider, E. (2000) *J. Bacteriol.* **182**, 1432–1436
- Treptow, N., and Shuman, H. (1985) *J. Bacteriol.* **163**, 654–660
- Covitz, K. M. Y., Panagiotidis, C. H., Hor, L. I., Reyes, M., Treptow, N. A., and Shuman, H. A. (1994) *EMBO J.* **13**, 1752–1759
- Panagiotidis, C. H., and Shuman, H. A. (1998) in *ABC Transporters: Biochemical* (Ambudkar, S. V., and Gottesman, M. M., eds) Vol. 292, pp. 30–39, Academic Press, San Diego, CA
- Schmees, G., and Schneider, E. (1998) *J. Bacteriol.* **180**, 5299–5305
- Vale, R. D. (1996) *J. Cell Biol.* **135**, 291–302
- Zdych, E., Peist, R., Reidl, J., and Boos, W. (1995) *J. Bacteriol.* **177**, 5035–5039
- Schreiber, V., Steegborn, C., Clausen, T., Boos, W., and Richet, E. (2000) *Mol. Microbiol.* **35**, 765–776
- Clausen, T., Schlegel, A., Peist, R., Schneider, E., Steegborn, C., Chang, Y.-S., Haase, A., Bourenkov, G. P., Bartunik, H. D., and Boos, W. (2000) *EMBO J.* **19**, 831–842
- Feese, M., Pettigrew, D. W., Meadow, N. D., Roseman, S., and Remington, S. J. (1994) *Proc. Natl. Acad. Sci. U. S. A.* **91**, 3544–3548
- Feese, M. D., Comolli, L., Meadow, N. D., Roseman, S., and Remington, S. J. (1997) *Biochemistry* **36**, 16087–16096
- Hurley, J. H., Faber, H. R., Worthylake, D., Meadow, N. D., Roseman, S., Pettigrew, D. W., and Remington, S. J. (1993) *Science* **259**, 673–677
- van der Vlag, J., van Dam, K., and Postma, P. W. (1994) *J. Bacteriol.* **176**, 3518–3526
- Wilken, S., Schmees, G., and Schneider, E. (1996) *Mol. Microbiol.* **22**, 655–666
- Schmees, G., Stein, A., Hunke, S., Landmesser, H., and Schneider, E. (1999) *Eur. J. Biochem.* **266**, 420–430
- Chang, G., and Roth, C. B. (2001) *Science* **293**, 1793–1800
- Laskowski, R. A., MacArthur, M. W., Moss, D. S., and Thornton, J. M. (1993) *J. Appl. Crystallogr.* **26**, 283–291
- Ramachandran, G. N., Ramakrishnan, C., and Sasisekharan, V. (1963) *J. Mol. Biol.* **7**, 95–99
- Engh, R., and Huber, R. (1991) *Acta Crystallogr. Sect. A* **47**, 392–400
- Hoof, R. W., Vriend, G., Sander, C., and Abola, E. E. (1996) *Nature* **381**, 272
- Vriend, G., and Sander, C. (1993) *J. Appl. Crystallogr.* **26**, 47–60
- Morris, A. L., MacArthur, M. W., Hutchinson, E. G., and Thornton, J. M. (1992) *Proteins* **12**, 345–364
- Verdon, G., Albers, S.-V., Driessen, A. J. M., Dijkstra, B., and Tunissen, A. M. (2001) *Acta Crystallogr. D*, in press